Protein-bound uremic toxin kinetics modeling for a new dialysis device

Kailei Liu

A thesis

submitted in partial fulfillment of the

requirements for the degree of

Master of Science

University of Washington

2020

Reading Committee:

Jim Pfaendtner

David Beck

Program Authorized to Offer Degree:

Chemical Engineering

University of Washington

Abstract

Protein-bound uremic toxin kinetics modeling for a new dialysis device

Kailei Liu

Chair of the Supervisory Committee:
Jim Pfaendtner
Department of Chemical Engineering

Addition to the conventional hemodialysis, a protein-bound uremic toxins process device is designed. To better understand the mechanism of this novel device, we build a fixed-bed adsorbent column model to simulate this process. Also, we build a compatible hemodialysis model with Python language. This hemodialysis model consists of a three-compartment patient model, a dialyzer model and toxin removal unit models where the PBUTs adsorption model can be plugged in. With these models, the effect of various parameters affecting adsorption process are discussed in detail.

TABLE OF CONTENTS

LIST OF FIGURES

LIST OF TABLES

ACKNOWLEDGEMENTS

I would like to acknowledge and thank my PI, Prof. Jim Pfaendtner, for his patience, encouragement and inspiration on this project. Thank you for providing me the opportunity to study in data science and to work with those outstanding researchers. Also, I would appreciate all the post-docs and students in PRG for sharing your knowledge and ideas. To all the staffs in CDI, I would like to say thank you for providing this novel project. I would like to thank the developers of FEniCS project and all the other developers who selflessly share their open-source Python packages. Most of all, I would like to thank all my family who would always support my choice and help me get through hard time.

Chapter 1. INTRODUCTION

1.1 FIXED BED ADSORBENT COLUMN

Conventional hemodialysis is a widely accepted therapy in kidney diseases. The massive difference between the concentration of uremic toxins in plasma and in dialysate leads to a large enough osmotic pressure and this will provide a rapid diffusion through the membrane. However, the conventional hemodialysis is less efficient in case of removing protein-bound uremic toxins (PBUTs). These toxins are bound to proteins in a high level, such as indoxyl sulfate (IS) and p-cresyl sulfate (pCS) have 90-98% bind to albumin [1], thus few free molecules remain in plasma and decrease the concentration gradient. For healthy person, the combination of protein-bounding mechanism and tubular secretion can reduce the unbound concentration. However, the uremic syndrome leads to the accumulation of PBUTs, e.g. IS and pCS are 116-fold and 41-fold greater compared to normal subjects. As a comparison, the predialysis concentration of urea is only 5-fold [2].

Several methods have been applied to improve the clearance of middle molecular weight molecules and PBUTs. Hemodiafiltration (HDF) combines convection and diffusion and shows superior effect on removal of p-cresol [3]. Dilution, higher temperature and increasing ionic strength have positive influence on indoxyl sulfate clearance since equilibrium is shifted to unbinding [4]. Adsorption onto synthetic membranes and microporous adsorbents enhance the elimination at high adsorption level [5]. Competitive displacer such as ibuprofen, furosemide and tryptophan can compete with PBUTs when binding to albumins [6]. Center for dialysis innovation at University of Washington designed a portable dialysis device, including a plug-in PBUTs processing device. Thus, we adopt fixed bed adsorption column model as the PBUTs removal part of the new device. To better understand the clearance of toxins, we build a mathematical kinetic model to demonstrate breakthrough curves.

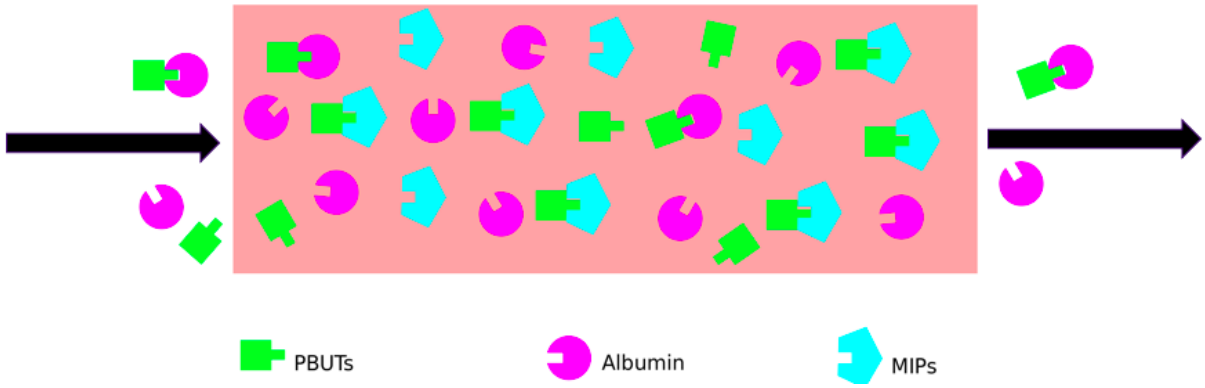

Figure 1. Schematic diagram showing plasma flow through fixed-bed adsorbent column

1.2 MODULAR HEMODIALYSIS MODEL

We are also interested in developing an expandable mathematical model simulating both patient and dialyzer. Maheshwari *et al.* reported a comprehensive hemodialysis model composed of a three-compartment patient model and a dialyzer model [7]. This proposed model is specially designed for protein-bound molecules. Compared to the conventional two-compartment patient model, it considers the unequal distribution of albumin in intracellular, interstitial and plasma compartment. This character of protein leads to the unique distribution of PBUTs. As for urea, this small molecular weight toxin does not bind to protein, so a two-compartment model can well describe the distribution of urea in physiological compartments [8]. We use Python language to build a modular hemodialysis model based on three-compartment patient model. This model has compatibility of two-compartment model when simulating urea clearance and expandability of various toxins processors.

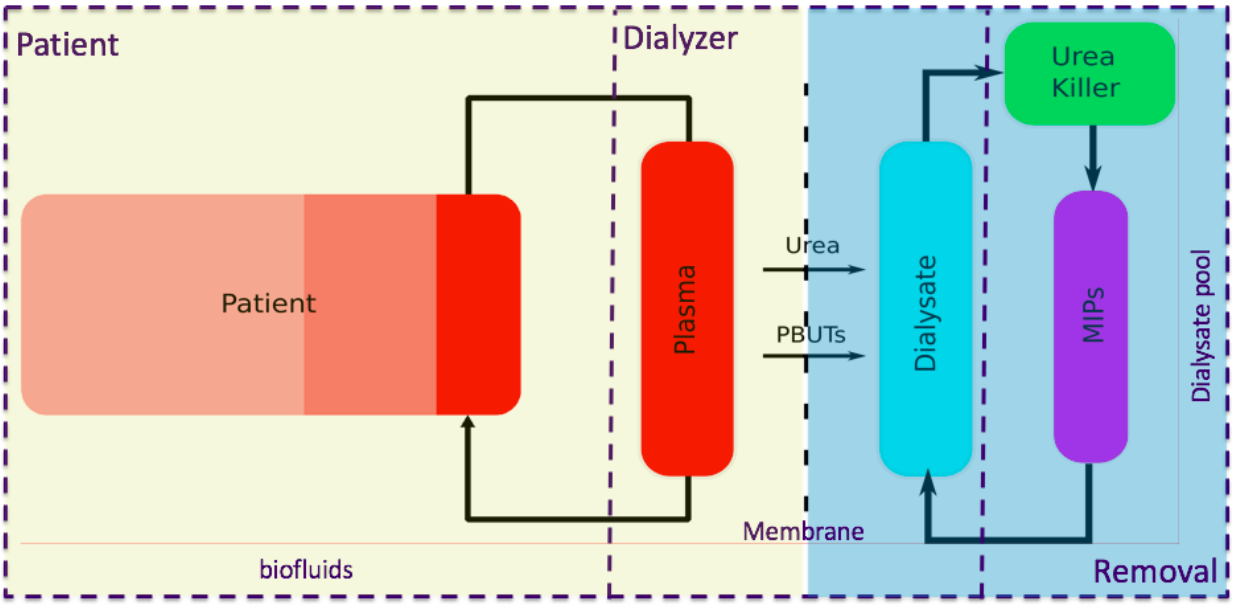

Figure 2. Block diagram of the hemodialysis model. Including a three-compartment model, a dialyzer model and toxin removal unit models

Chapter 2. MATHEMATICAL MODELING

2.1 FIXED-BED ADSORBENT MODEL

This packed bed adsorption model is described by three diffusion equations, and all of them are solved by numeric method. Based on this mathematical model, breakthrough curve and concentration versus length curve can be predicted. Also, we are interested in the change of curves regarding to different parameters. Finally, the most appropriate values of the parameters will be adopted and be used in further study. To solve these governing equations, there are some assumptions [9]:

1. Axial dispersion is negligible in this system.
2. Velocity of the flow remains constant.
3. There is no concentration gradient in the radical direction in bulk fluid.
4. The particles are spherical and identical in size and weight.
5. The Linear Driving Force (LDF) model is adopted to express intrapellet diffusion rate with concentration in solid phase.

6. The optimal isotherm model is Langmuir model, but linear model can also be used in this dilute system.

With the above assumptions, the governing equation of free toxin, unbinding protein and binding protein along with initial conditions can be written:

Fluid phase mass balance

$$\frac{\delta c_T}{\delta t} + \frac{(1-\varepsilon)}{\varepsilon}\rho_s \frac{\delta \bar{q}}{\delta t}\frac{10^6}{M} + u\frac{\delta c_T}{\delta z} = k_{on}c_P c_T - k_{off}c_{PT} \tag{2.1.1}$$

$$\frac{\delta c_P}{\delta t} + u\frac{\delta c_P}{\delta z} = k_{on}c_P c_T - k_{off}c_{PT} \tag{2.1.2}$$

$$\frac{\delta c_{PT}}{\delta t} + u\frac{\delta c_{PT}}{\delta z} = -k_{on}c_P c_T + k_{off}c_{PT} \tag{2.1.3}$$

Where ε is the void factor and ρ_s is the density of adsorbent.

In the equation (2.1.1), the first item represents the toxin concentration in fluid phase. The next item is the amount of toxin adsorbed by MIPs. Then the item containing velocity represents the convective mass transfer. And the right side of the equation is the reaction rate of toxin-protein bound.

Initial and boundary conditions

$$c|_{t=0,z>0} = 0 \tag{2.1.4}$$

$$c|_{t\geq 0,z=0} = c_{in} \tag{2.1.5}$$

The rate of solid loading is represented by LDF model

$$\frac{\delta \bar{q}}{\delta t} = k_e(q_s - \bar{q}) \tag{2.1.6}$$

Where k_e is the intrapellet diffusion kinetic coefficient, q_s is the solid face concentration in the surface of adsorbent particle and $\bar{q}$ is the average concentration of the toxin. In most case, the diffusion coefficient can be expressed by solid diffusion coefficient D_s and the radius of particles R.

$$k_e = \frac{15D_s}{R^2} \tag{2.1.7}$$

The concentration gradient in the interface region between fluid phase and MIPs may not be neglected, so the external mass transfer is given by

$$\frac{\delta \bar{q}}{\delta t} = \frac{3k_f}{R}(c_b - c_s) \tag{2.1.8}$$

Where k_f is the mass transfer coefficient, c_b is the bulk concentration and c_s represents the concentration at the fluid-adsorbent interface.

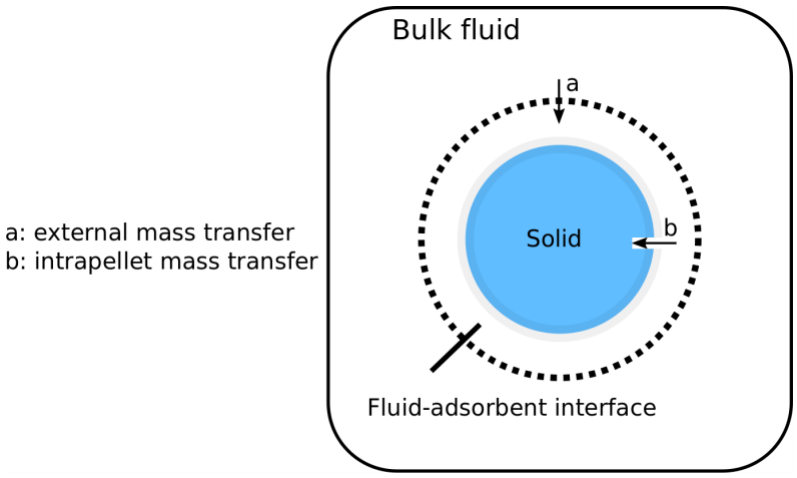

Figure 3. Adsorption process of an adsorbent particle [30]

As far as the system is in equilibrium state, the c_s and q_s can be obtained by using isotherm models. There are two kinds of isotherm model suit for numerical method – linear isotherm

$$\rho_s q_s = H c_s \tag{2.1.9}$$

where H is similar to Henry's constant,

and Langmuir isotherm (Figure 4)

$$q_s = q_{max} \cdot \frac{K c_s}{1 + K c_s} \tag{2.1.10}$$

where q_{max} is the capacity of the adsorbent and K is the Langmuir isotherm parameter.

Differentiate q_s with surface concentration c_s

$$\frac{dq_s}{dc_s} = \frac{q_{max} K}{(1 + K c_s)^2} \tag{2.1.11}$$

When the dialysate is a dilute solution for free toxin, the equation (2.1.11) can be regarded as a constant $q_{max}K$. Which means in a dilute solution, the linear isotherm and the Langmuir isotherm are equivalent, where $H = \rho_s \cdot q_{max} \cdot K$. However, to obtain a better accuracy, the Langmuir isotherm outweighs the other one.

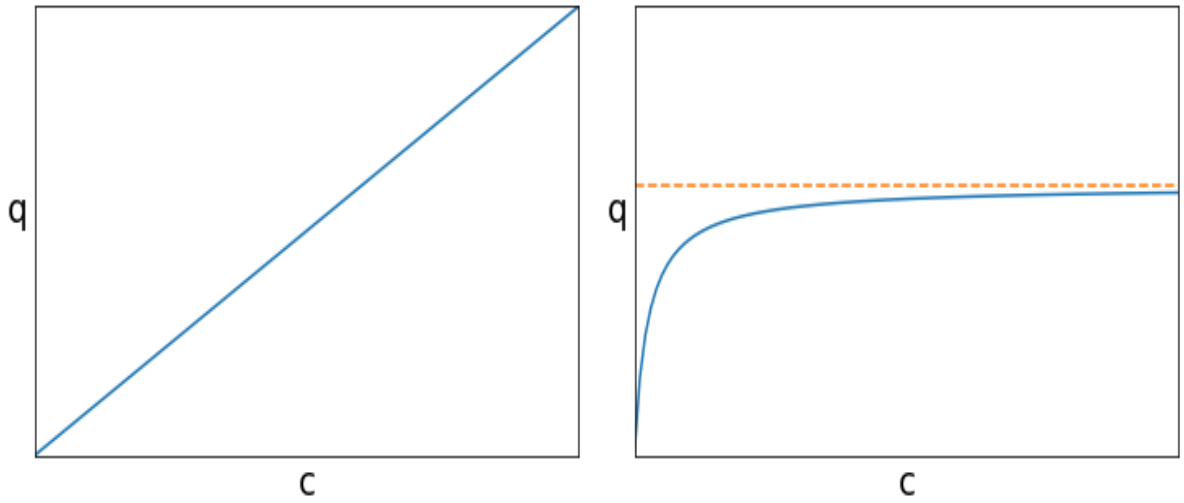

Figure 4. Linear Isotherm and Langmuir Isotherm

Combine equation (2.1.6), (2.1.7) and (2.1.8) to solve q_s with measurable c_b

$$q_s - \bar{q} = \frac{Bi}{5\rho}(c_b - c_s) \tag{2.1.12}$$

where $Bi = \frac{k_f}{RD_s}$ is Biot number.

Then differentiate equation (2.1.12) with time for both sides [10]

$$\frac{dq_s}{dt} - \frac{d\bar{q}}{dt} = \frac{Bi}{5\rho}\left(\frac{\partial c_b}{\partial t} - \frac{dc_s}{dq_s} \cdot \frac{dq_s}{dt}\right) \tag{2.1.13}$$

Rearrange equation (2.1.13) and substitute with equation (2.1.10)

$$\frac{\partial q_s}{\partial t} = \frac{\frac{3k_f}{R\rho}\left(c_b - \frac{q_s}{K(q_{max} - q_s)}\right) + \frac{Bi}{5\rho}\frac{\partial c_b}{\partial t}}{1 + \frac{Bi}{5\rho} \cdot \frac{q_{max}}{K(q_{max} - q_s)^2}} \tag{2.1.14}$$

Equation (2.1.14) can also be solved by numerical method, and in this way, q_s in each step will be obtained.

Table 1. Nomenclature and parameters value for fixed-bed adsorbent column

Symbol	Description	Default Value/ Unit
ε	Void faction	0.58
H	Linear isotherm parameter	28
K	Langmuir isotherm parameter	1 ml/mg
Q	Dialysate flow rate	100 ml/min
u	Dialysate velocity	cm/min
d	Column diameter	4 cm
L	Column length	7.6 cm
ρ_s	Adsorbent density	0.7 g/ml
q_{max}	Capacity	40 mg/g
R	Particle radius	0.01 cm
k_f	External film mass transfer coefficient	1.5×10^{-6} m/s
D_s	Micropore diffusivity	2.5×10^{-8} m^2/s
c_b	Bulk concentration	mg/ml
c_s	Surface concentration in fluid phase	mg/ml
q_s	Surface concentration in solid phase	mg/g
$\bar{q}$	Average concentration in particle	mg/g
c_{t_in}	Free toxin inlet concentration	μM
c_{p_in}	Unbinding protein inlet concentration	μM
c_{pt_in}	Binding protein inlet concentration	μM
k_{on}	Binding reaction rate	$36\ min^{-1}\cdot\mu M^{-1}$
k_{off}	Decomposition reaction rate	$2040\ min^{-1}$

2.2 HEMODIALYSIS MODEL

This three-compartment patient model is governed by a system of seven ordinary differential equations [7].

For intracellular part, the pool volume is considered to be constant

$$\frac{d(V_{ic}C_{t,ic})}{dt} = G - K_{ic,T}(C_{t,ic} - C_{t,is}) \tag{2.2.1}$$

Toxin generate in this compartment and transfer into interstitial pool.

For Interstitial pool, a small amount of fluid will be removed during the dialysis. So, there is convective diffusion term in the equations and the volume decrease with time

$$\frac{d(V_{is}C_{t,is})}{dt} = K_{ic,T}(C_{t,ic} - C_{t,is}) - K_{ip,T}(C_{t,is} - C_{t,pl}) - \alpha Q_{uf}C_{t,is} + (-k_1 C_{p,is}C_{t,is} + k_2 C_{pt,is})V_{is} \tag{2.2.2}$$

$$\frac{d(V_{is}C_{pt,is})}{dt} = (k_1 C_{p,is}C_{t,is} - k_2 C_{pt,is})V_{is} \tag{2.2.3}$$

$$\frac{d(V_{is}C_{p,is})}{dt} = (-k_1 C_{p,is}C_{t,is} + k_2 C_{pt,is})V_{is} \tag{2.2.4}$$

Protein and toxin-protein complex will not transfer through membrane so that the concentration is only affected by bind-unbind reaction.

For plasma pool, volume also varies with time. Here, the outlet concentrations are parameters governed by dialyzer model

$$\frac{d(V_{pl}C_{t,pl})}{dt} = -Q_p C_{t,pl} + (Q_p - Q_{uf})C_{t,out} + K_{ip,T}(C_{t,is} - C_{t,pl}) + \alpha Q_{uf}C_{t,is} + (-k_1 C_{p,pl}C_{t,pl} + k_2 C_{t,pl})V_{pl} \tag{2.2.5}$$

$$\frac{d(V_{pl}C_{pt,pl})}{dt} = -Q_p C_{pt,pl} + (Q_p - Q_{uf})C_{pt,out} + (k_1 C_{p,pl}C_{t,pl} - k_2 C_{t,pl})V_{pl} \tag{2.2.6}$$

$$\frac{d(V_{pl}C_{p,pl})}{dt} = -Q_p C_{p,pl} + (Q_p - Q_{uf})C_{p,out} + (-k_1 C_{p,pl}C_{t,pl} + k_2 C_{t,pl})V_{pl} \tag{2.2.7}$$

Volume decreases at a constant rate

$$\frac{dV_{is}}{dt} = -\alpha Q_{uf} \tag{2.2.8}$$

$$\frac{dV_{pl}}{dt} = -(1-\alpha)Q_{uf} \tag{2.2.9}$$

$$\alpha = \frac{V_{is}}{V_{is}+V_{pl}} \tag{2.2.10}$$

Although both V_{is} and V_{pl} vary from time, it can be easily proved that α is a constant.

Differentiate equation (2.2.10) with time t

$$\frac{d\alpha}{dt} = \frac{(V_{is}+V_{pl})\frac{dV_{is}}{dt} - V_{is}\frac{d(V_{is}+V_{pl})}{dt}}{(V_{is}+V_{pl})^2}$$

$$= \frac{V_{pl}\frac{dV_{is}}{dt} - V_{is}\frac{dV_{pl}}{dt}}{(V_{is}+V_{pl})^2} \tag{2.2.11}$$

Substitute equation (2.2.8) and (2.2.9) into (2.2.11), we will find

$$\frac{d\alpha}{dt} = 0 \tag{2.2.12}$$

To get the values of outlet concentrations, we need to solve the dialyzer model. This is a system of four partial differential equations

Blood side

$$\frac{\partial C_t}{\partial t} = -\frac{1}{NA}\frac{\partial}{\partial x}(Q_p C_t) - \frac{1}{NAL}\left(K_0 A(C_t - C_{t,d}) + Q_{uf}\overline{C_t}\right) + \left(-k_1 C_t C_p + k_2 C_{pt}\right) \tag{2.2.13}$$

$$\frac{\partial C_{pt}}{\partial t} = -\frac{1}{NA}\frac{\partial}{\partial x}(Q_p C_{pt}) + \left(k_1 C_t C_p - k_2 C_{pt}\right) \tag{2.2.14}$$

$$\frac{\partial C_p}{\partial t} = -\frac{1}{NA}\frac{\partial}{\partial x}(Q_p C_p) + \left(-k_1 C_t C_p + k_2 C_{pt}\right) \tag{2.2.15}$$

Dialysate side

$$\frac{\partial C_{t,d}}{\partial t} = \frac{1}{NA_d}\frac{\partial}{\partial x}(Q_d C_{t,d}) + \frac{1}{NA_d L_d}\left(K_0 A(C_t - C_{t,d}) + Q_{uf}\overline{C_t}\right) \tag{2.2.16}$$

Plasma flow through the fibers while dialysate flow through the surrounding area in the opposite direction. $\overline{C_t}$ denotes the toxin concentration inside membranes where convective transfer happens.

$$\overline{C_t} = C_t(1-\varphi) + C_{t,d}\varphi \tag{2.2.17}$$

$$\varphi = \frac{1}{Pe} - \frac{1}{e^{Pe}-1} \tag{2.2.18}$$

where $Pe = \frac{Q_{uf}}{K_0 A}$ is Péclet number

During the dialysis, the plasma flow rate decreases along the fiber due to ultrafiltration, while the dialysate flow rate increases

$$Q_p(x) = Q_{pi} - \frac{x}{L_d}Q_{uf} \tag{2.2.19}$$

$$Q_d(x) = Q_{di} + \frac{L_d - x}{L_d}Q_{uf} \tag{2.2.20}$$

The boundary condition for the first three PDEs is dynamic. The value of inlet concentrations equal to the relevant plasma concentrations, which means they vary with time and governed by the patient model.

Table 2. Nomenclature and parameters value for hemodialysis model [7].

Symbol	Description	Default Value/ Unit
G	Toxin generation rate	mg/min
$K_{ic,T}$	Toxin mass transfer coefficient between intracellular and interstitial pool	ml/min
$K_{ip,T}$	Toxin mass transfer coefficient between interstitial and plasma pool	ml/min
V_{ic}	Volume of intracellular pool	25.9L
V_{is}	Volume of interstitial pool	10.5L
V_{pl}	Volume of plasma pool	2.4L

α	Fraction of interstitial compartment in extracellular fluid	-
k_1	Binding reaction rate	36 min^{-1} · μM^{-1}
k_2	Decomposition reaction rate	2040 min^{-1}
$C_{t,ic}$	Toxin concentration in intracellular compartment	μM
$C_{t/p/pt,is}$	Toxin/ protein/ toxin-protein complex concentration in interstitial compartment	μM
$C_{t/p/pt,pl}$	Toxin/ protein/ toxin-protein complex concentration in plasma compartment	μM
$C_{t/p/pt,out}$	Toxin/ protein/ toxin-protein complex concentration flow out from dialyzer	μM
$Q_{p/d/uf}$	Flow rate in blood/ dialysate/ ultrafiltration	ml/min
$Q_{pi/di}$	Initial flow rate of blood/ dialysate in dialyzer	ml/min
$C_{t/p/pt}$	Toxin/ protein/ toxin-protein complex concentration in dialyzer	μM
$C_{t,d}$	Toxin concentration in dialysate	μM
K_0A	Dialyzer mass transfer-area coefficient	600 ml/min
N	Number of fibers	12300
A	Blood flow area of a single fiber	3.5×10^{-4} cm^2
A_d	Dialysate flow area around a single fiber	4.06×10^{-4} cm^2
L_d	Length of fibers in dialyzer	23 cm

Chapter 3. SIMULATION TECHNIQUE

The set of partial differential equation (2.1.1 to 2.1.14) is solved by explicit finite difference method. Since the model is regarded as a one-dimensional mass transfer problem, we divide the column into several nodes and calculate the concentration on each node from step to step [11]. The mathematic algorithm is developed with Python 3.6.8.

Table 3. Toxin parameters value [31]. During the simulation, the concentration is normalized. So the most common used unit is adopted

Toxin	Type	$K_{ic,T}$ (ml/min)	$K_{ip,T}$ (ml/min)	k_1 (min^{-1} · μM^{-1})	G (mg/min)	C_*
urea	Non-PBUT	363	-	-	0.0285	10 μM
Indoxyl sulfate	PBUT	103	1210	36	8.17	0.95 mg/ml

As for hemodialysis model, values of outlet concentration (these are parameters rather than unknowns) in three-compartment patient model and the boundary conditions for blood side of dialyzer model are both time-dependent and determined by each other. Thus, solution to the hemodialysis model is also under the concept of explicit finite difference to obtain the values of parameters and boundary conditions. However, during each time step, standard solutions are applied to these two sets of differential equations. Ordinary differential equations (2.2.1 to 2.2.12) are solved with open source Python module Scipy.integrate.solve_ivp [12-25]. Partial differential equations (2.2.13 to 2.2.20) are solved with standard PDE solver FEniCS Project [26-29]. This open-source software provides finite element method programming in Python. In case of urea clearance, we do not simulate the removal process. So, we assume 95% urea are successfully removed. In case of PBUTs clearance, we adopt fixed-bed adsorbent column as the removal unit. However, since protein and toxin-protein complex do not transfer through dialyzer, only toxins flow through the column. In this way, the item of reaction rate in equation (2.2.1) is neglected. The solution of fixed-bed adsorbent column model provides the boundary condition for dialysate side of dialyzer model.

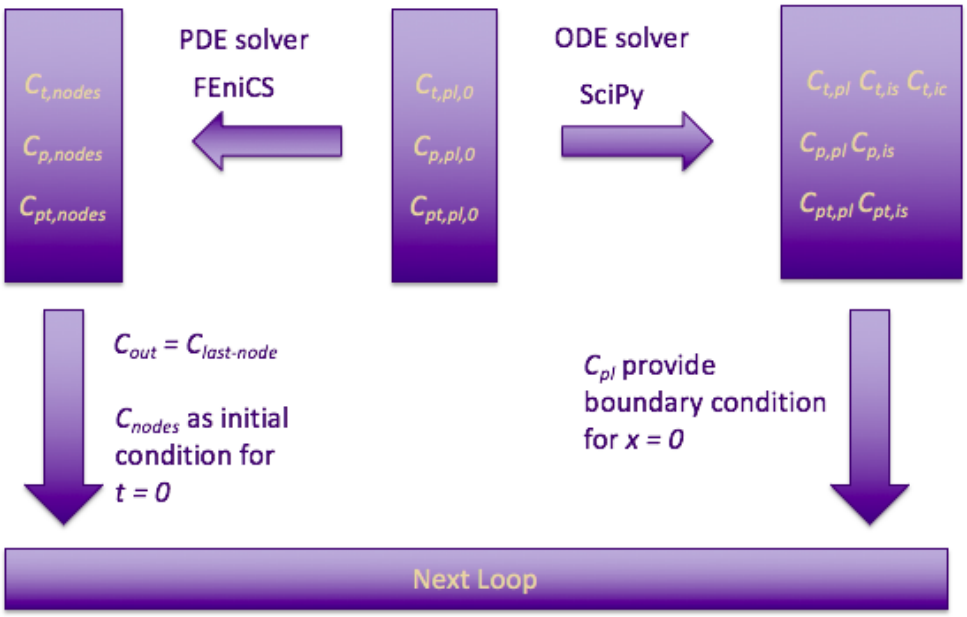

Figure 5. Schematic diagram showing the calculation process in a single time step. Toxin removal units are not included.

Chapter 4. RESULT AND DISCUSSION

4.1 EFFECT OF ISOTHERM PARAMETER

The effect of isotherm parameter is shown in Figure 6. During this simulation, we use linear equilibrium isotherm to simplify the calculation. Figure 6(a) shows the breakthrough curve is not affected by isotherm parameter. However, Figure 6(b) shows by increasing isotherm parameter, more toxin will be absorbed. As we discussed in chapter 2.1, linear isotherm is the approximation of Langmuir isotherm in dilute solution. Langmuir isotherm is obtained under the assumption of second-order reaction and is defined by the equilibrium constant. So, it suggests that a stronger binding between adsorbent and toxin molecules will lead to a larger amount of adsorption.

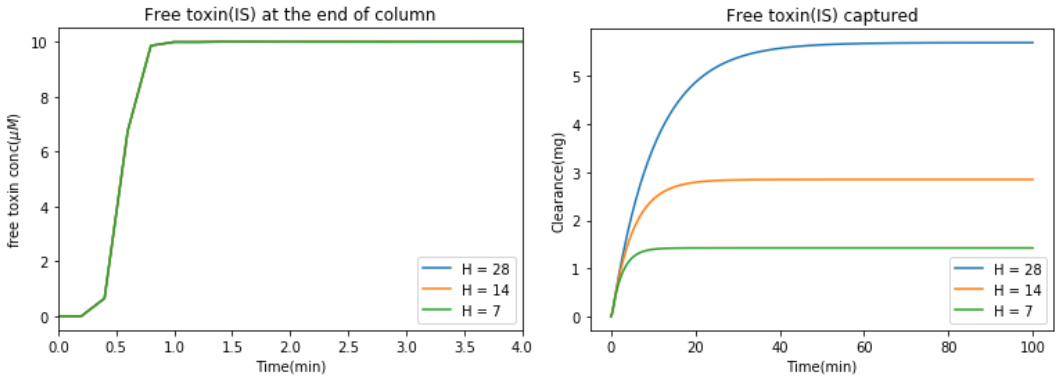

Figure 6. (a) Breakthrough curve and (b) amount of clearance with various of isotherm parameters

4.2 EFFECT OF FLOW RATE

The effect of flow rate is shown in Figure 7. The flow rate is considered 50 ml/min, 100 ml/min and 200 ml/min respectively. It is shown in Figure 7(a) that breakthrough point appears earlier with larger flow rate. Although Figure 7(b) suggests larger flow rate may increase the uptake rate, Figure 7(c) shows the total amount of capture remain steady with various of flow rate.

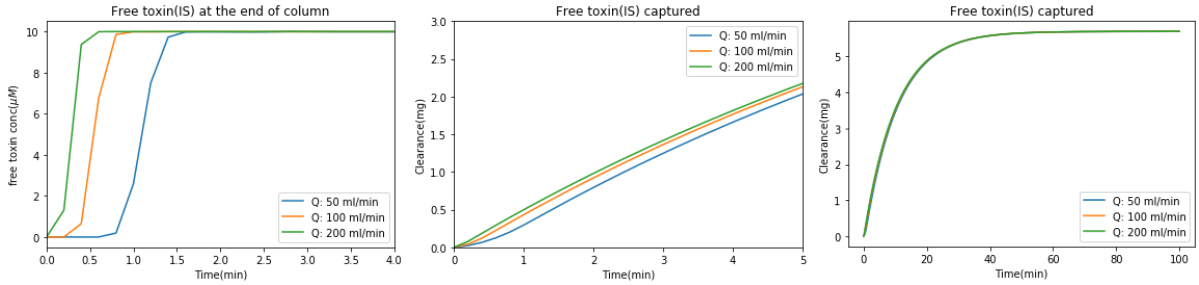

Figure 7. (a) Breakthrough curve and (b) (c) amount of clearance with various of flow rate

4.3 EFFECT OF PARTICLE CAPACITY

The effect of adsorbent capacity is shown in Figure 8. The upper panel of plots show that curves are independent with capacity. However, there is no physical meaning in keep *H* constant. As stated above, a constant *K* suggests the uniform strength of adsorbent binding. Thus, in the lower panel we simulate with the identical Langmuir isotherm. They show the particle capacity only affect the amount of toxin adsorption.

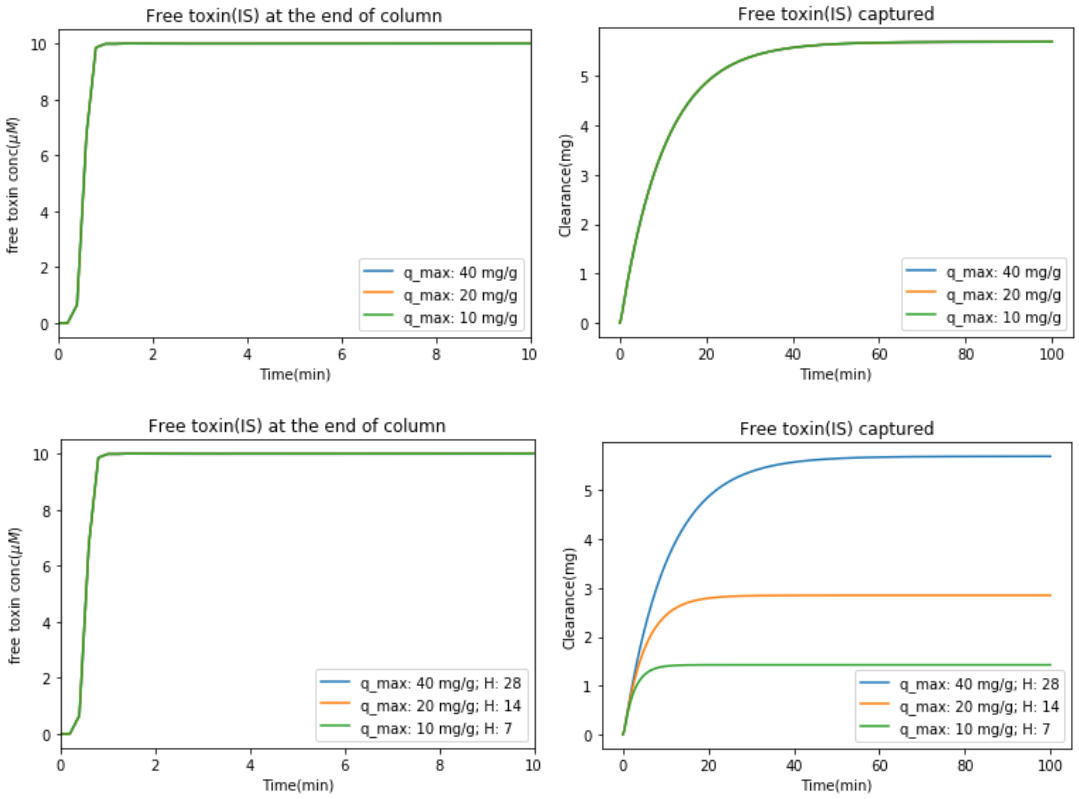

Figure 8. (a) Breakthrough curve and (b) amount of clearance with various of capacity and a constant *H*; (c) Breakthrough curve and (d) amount of clearance with various of capacity and a constant *K*

4.4 EFFECT OF PARTICLE RADIUS

The effect of adsorbent size is shown in Figure 9. There is no significant change in breakthrough curve with different radius. But in Figure 9(b), that uptake rate is affected by various radius and the final amount of adsorption seems to remain constant. It may be explained that the smaller the particle, the larger the specific surface area, which leads to a faster adsorption.

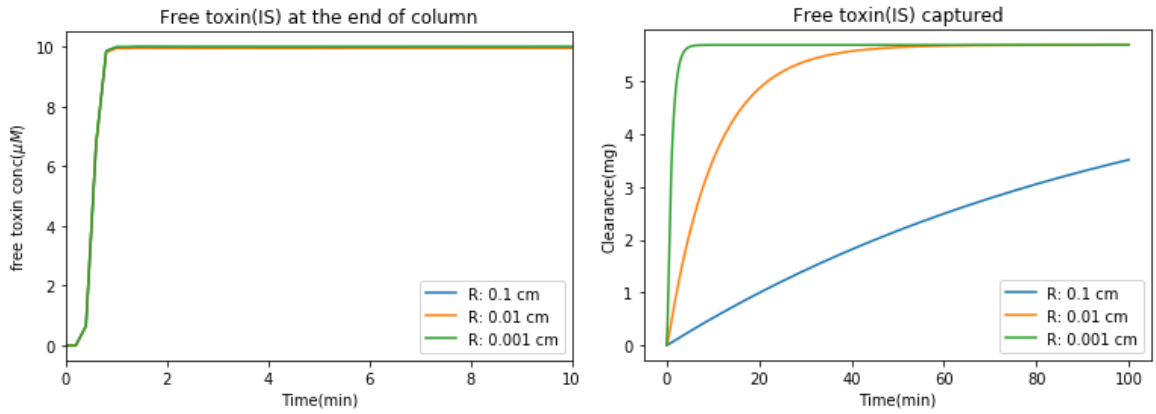

Figure 9. (a) Breakthrough curve and (b) amount of clearance with various of particle radius

4.5 EFFECT OF COLUMN LENGTH

The effect of column length is shown in Figure 10. Apparently, breakthrough point appears later in a longer column. Also, a longer column contains more adsorbent and will eventually adsorb more toxin molecules.

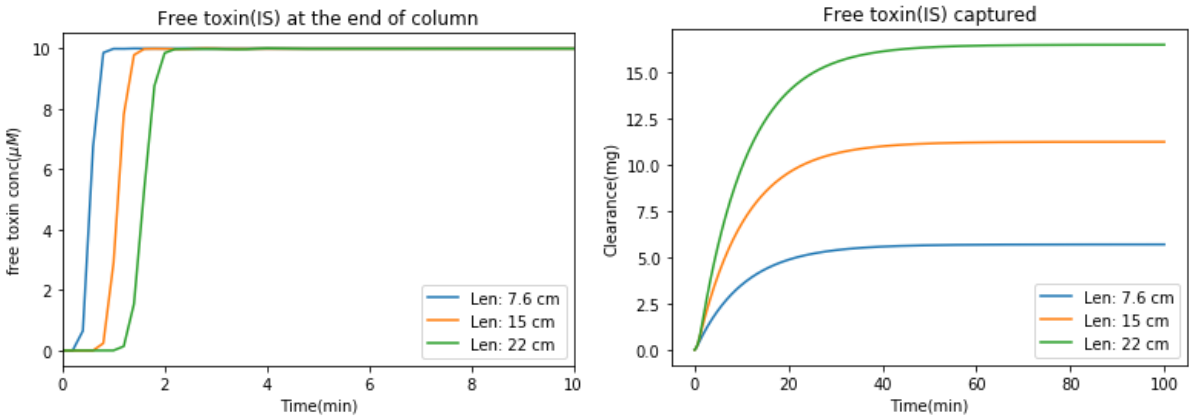

Figure 10. (a) Breakthrough curve and (b) amount of clearance with various of column length

4.6 EFFECT OF EXTERNAL FILM MASS TRANSFER COEFFICIENT

The effect of external film mass transfer coefficient k_f is shown in Figure 11. The result shows a similar influence as the effect of particle radius. The external mass transfer coefficient is estimated with the following correlation [32]

$$Sh = \frac{2k_f R}{D_m} = 2 + 1.1Sc^{\frac{1}{3}}Re^{0.6} \quad (4.6.1)$$

Where *Sh* is Sherwood number, *Sc* is Schmidt number and *Re* is Reynolds number.

It suggests that external film mass transfer coefficient can be affected by adsorbent radius, toxin molecular diffusivity and fluid viscosity, which can be adjusted by developing different adsorbent materials.

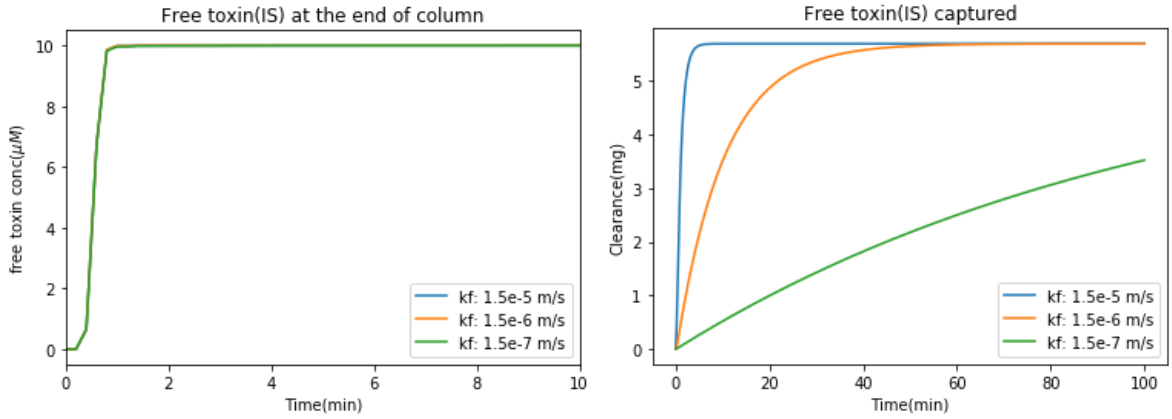

Figure 11. (a) Breakthrough curve and (b) amount of clearance with various of k_f

4.7 RESULT OF UREA AND INDOXYL SULFATE SIMULATION

The unequal distribution of toxins in each compartment can be observed in Figure 12. For indoxyl sulfate, the concentration in plasma drops the most. For urea, concentration in plasma and interstitial pools are identical. These simulations are displayed with the same hemodialysis model but different toxin properties and toxin removal unit models.

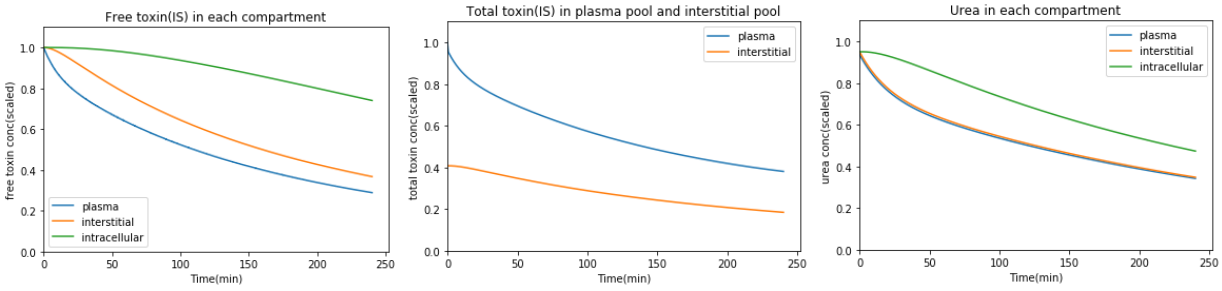

Figure 12. (a) free IS concentration in three compartments, (b) total IS concentration in plasma and interstitial compartment, (c) urea concentration in three compartments

Chapter 5. CONCLUSION

A fixed-bed adsorbent column model is developed and solved with numeric method. This model can also be plugged into a compatible hemodialysis model. Furthermore, Effects of various parameters on breakthrough curve and adsorption curve are discussed. We observe that the flow rate and the length of column will affect the breakthrough curve. Also, Isotherm parameter, particle capacity and the length of column will affect the amount of adsorption. Flow rate as well as the radius of particle and external film mass transfer coefficient only affect the uptake rate.

BIBLIOGRAPHY

[1] Sirich, Tammy L., et al. "Protein-bound molecules: a large family with a bad character." *Seminars in nephrology*. Vol. 34. No. 2. WB Saunders, 2014.

[2] Sirich, Tammy L., et al. "Prominent accumulation in hemodialysis patients of solutes normally cleared by tubular secretion." Journal of the American Society of Nephrology25.3 (2014): 615-622.

[3] Bammens, Bert, et al. "Removal of the protein-bound solute p-cresol by convective transport: a randomized crossover study." American journal of kidney diseases 44.2 (2004): 278-285.

[4] Devine, Eric, et al. "Binding affinity and capacity for the uremic toxin indoxyl sulfate." Toxins 6.2 (2014): 416-429.

[5] Wernert, Véronique, et al. "Adsorption of the uremic toxin p-cresol onto hemodialysis membranes and microporous adsorbent zeolite silicalite." Journal of biotechnology 123.2 (2006): 164-173.

[6] Tao, Xia, et al. "Improved dialytic removal of protein-bound uraemic toxins with use of albumin binding competitors: an in vitro human whole blood study." Scientific reports 6.1 (2016): 1-9.

[7] Maheshwari, Vaibhav, et al. "A novel mathematical model of protein-bound uremic toxin kinetics during hemodialysis." Scientific reports 7.1 (2017): 1-15.

[8] Clark, William R., et al. "Quantifying the effect of changes in the hemodialysis prescription on effective solute removal with a mathematical model." Journal of the American Society of Nephrology 10.3 (1999): 601-609.

[9] Babu, B. V., and Suresh Gupta. "Modeling and simulation for dynamics of packed bed adsorption." Proceedings of international symposium & 57th annual session of IIChE in association with AIChE (CHEMCON-2004), Mumbai. 2004.

[10] Markovska, L., et al. "Solid diffusion control of the adsorption of basic dyes onto granular activated carbon and natural zeolite in fixed bed columns." Journal of the Serbian Chemical Society 66.7 (2001): 463-475.

[11] Chapra, Steven C., and Raymond P. Canale. Numerical methods for engineers. Boston: McGraw-Hill Higher Education,, 2010.

[12] J. R. Dormand, P. J. Prince, “A family of embedded Runge-Kutta formulae”, Journal of Computational and Applied Mathematics, Vol. 6, No. 1, pp. 19-26, 1980.

[13] L. W. Shampine, “Some Practical Runge-Kutta Formulas”, Mathematics of Computation,, Vol. 46, No. 173, pp. 135-150, 1986.

[14] P. Bogacki, L.F. Shampine, “A 3(2) Pair of Runge-Kutta Formulas”, Appl. Math. Lett. Vol. 2, No. 4. pp. 321-325, 1989.

[15] E. Hairer, G. Wanner, “Solving Ordinary Differential Equations II: Stiff and Differential-Algebraic Problems”, Sec. IV.8.

[16] Backward Differentiation Formula on Wikipedia.

[17] L. F. Shampine, M. W. Reichelt, “THE MATLAB ODE SUITE”, SIAM J. SCI. COMPUTE., Vol. 18, No. 1, pp. 1-22, January 1997.

[18] C. Hindmarsh, “ODEPACK, A Systematized Collection of ODE Solvers,” IMACS Transactions on Scientific Computation, Vol 1., pp. 55-64, 1983.

[19] L. Petzold, “Automatic selection of methods for solving stiff and nonstiff systems of ordinary differential equations”, SIAM Journal on Scientific and Statistical Computing, Vol. 4, No. 1, pp. 136-148, 1983.**9**

[20] Stiff equation on Wikipedia.

[21] Curtis, M. J. D. Powell, and J. Reid, “On the estimation of sparse Jacobian matrices”, Journal of the Institute of Mathematics and its Applications, 13, pp. 117-120, 1974.

[22] Cauchy-Riemann equations on Wikipedia.

[23] Lotka-Volterra equations on Wikipedia.

[24] E. Hairer, S. P. Norsett G. Wanner, “Solving Ordinary Differential Equations I: Nonstiff Problems”, Sec. II.

[25] Page with original Fortran code of DOP853.

[26] Alnæs, Martin, et al. "The FEniCS project version 1.5." *Archive of Numerical Software* 3.100 (2015).

[27] Logg, Anders, Kent-Andre Mardal, and Garth Wells, eds. *Automated solution of differential equations by the finite element method: The FEniCS book*. Vol. 84. Springer Science & Business Media, 2012.

[28] Logg, Anders, and Garth N. Wells. "DOLFIN: Automated finite element computing." *ACM Transactions on Mathematical Software (TOMS)* 37.2 (2010): 1-28.

[29] Logg, Anders, Garth N. Wells, and Johan Hake. "DOLFIN: A C++/Python finite element library." *Automated solution of differential equations by the finite element method*. Springer, Berlin, Heidelberg, 2012. 173-225.

[30] Xu, Zhe, Jian-guo Cai, and Bing-cai Pan. "Mathematically modeling fixed-bed adsorption in aqueous systems." *Journal of Zhejiang University SCIENCE A* 14.3 (2013): 155-176.

[31] Eloot, Sunny, et al. "Protein-bound uremic toxin profiling as a tool to optimize hemodialysis." *PloS one* 11.1 (2016).

[32] Shafeeyan, Mohammad Saleh, Wan Mohd Ashri Wan Daud, and Ahmad Shamiri. "A review of mathematical modeling of fixed-bed columns for carbon dioxide adsorption." *Chemical engineering research and design* 92.5 (2014): 961-988.